

# PHOTOGRAMMETRY-DERIVED ORTHOIMAGERY AND ELEVATION DATA FOR KIPNUK, ALASKA, COLLECTED JUNE 21, 2022

Keith C. Horen, Richard M. Buzard, Jacquelyn R. Overbeck, Autumn C. Poisson, and Zachary J. Siemsen

Raw Data File 2024-14



Location maps showing the survey area.

This report has not been reviewed for technical content or for conformity to the editorial standards of DGGS.

2025 Update – Drone video added

2024  
STATE OF ALASKA  
DEPARTMENT OF NATURAL RESOURCES  
DIVISION OF GEOLOGICAL & GEOPHYSICAL SURVEYS



## **STATE OF ALASKA**

Mike Dunleavy, Governor

## **DEPARTMENT OF NATURAL RESOURCES**

John Boyle, Acting Commissioner

## **DIVISION OF GEOLOGICAL & GEOPHYSICAL SURVEYS**

Melanie Werdon, State Geologist & Director

Publications produced by the Division of Geological & Geophysical Surveys are available to download from the DGGS website ([dgg.alaska.gov](https://dgg.alaska.gov)). Publications on hard-copy or digital media can be examined or purchased in the Fairbanks office:

### **Alaska Division of Geological & Geophysical Surveys (DGGS)**

3354 College Road | Fairbanks, Alaska 99709-3707

Phone: 907.451.5010 | Fax 907.451.5050

[dggspubs@alaska.gov](mailto:dggspubs@alaska.gov) | [dgg.alaska.gov](https://dgg.alaska.gov)

### **DGGS publications are also available at:**

Alaska State Library, Historical  
Collections & Talking Book Center  
395 Whittier Street  
Juneau, Alaska 99801

Alaska Resource Library and  
Information Services (ARLIS)  
3150 C Street, Suite 100  
Anchorage, Alaska 99503

### **Suggested citation:**

Horen, K.C., Buzard, R.M., Overbeck, J.R., Poisson, A.C., and Siemsen, Z.J., 2024, Photogrammetry-derived orthoimagery and elevation data for Kipnuk, Alaska, collected June 21, 2022: Alaska Division of Geological & Geophysical Surveys Raw Data File 2024-14, 6 p. <https://doi.org/10.14509/31271>



# PHOTOGRAMMETRY-DERIVED ORTHOIMAGERY AND ELEVATION DATA FOR KIPNUK, ALASKA, COLLECTED JUNE 21, 2022

Keith C. Horen<sup>1</sup>, Richard M. Buzard<sup>2</sup>, Jacquelyn R. Overbeck<sup>1</sup>, Autumn C. Poisson<sup>1</sup>, and Zachary J. Siemsen<sup>1</sup>

## INTRODUCTION

The Alaska Division of Geological & Geophysical Surveys (DGGs) collected low-altitude aerial images and video from an unmanned aerial vehicle (UAV) in the community of Kipnuk, Alaska, on June 21, 2022. We used Structure-from-Motion (SfM) photogrammetry to produce a digital surface model (DSM) and orthoimagery (fig. 1). The orthoimage and elevation data are useful for assessing coastal hazards and changes over time. These products are released as a Raw Data File with an open end-user license. All files can be downloaded from [doi.org/10.14509/31271](https://doi.org/10.14509/31271) or [elevation.alaska.gov](https://elevation.alaska.gov).

## LIST OF DELIVERABLES

- Orthoimagery
- Digital Surface Model (DSM)
- Drone video\*
- Metadata

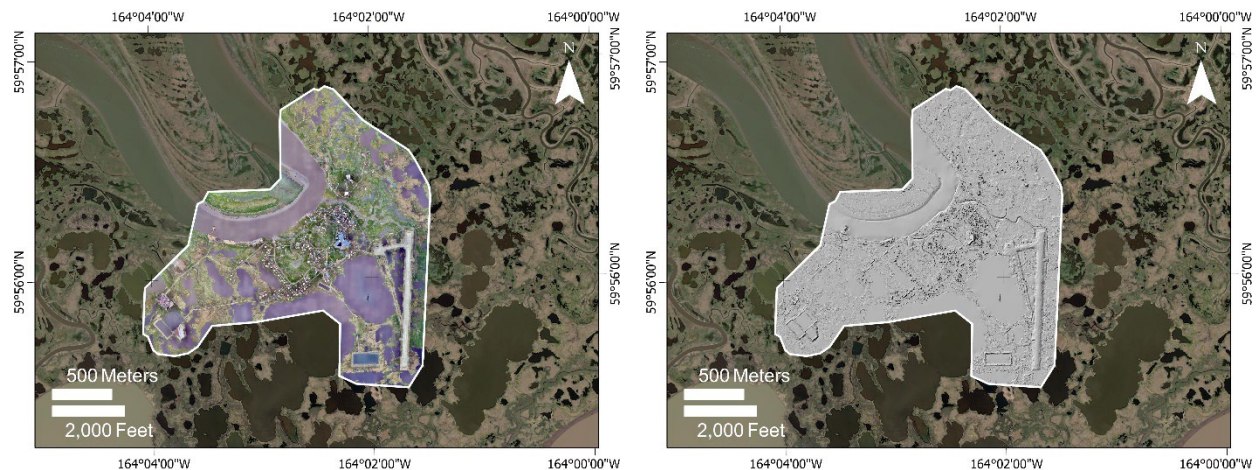


**Figure 1.** Extent of orthoimage (left) and digital surface model (DSM) (right) for Kipnuk.

<sup>1</sup> Alaska Division of Geological & Geophysical Surveys, 3354 College Road, Fairbanks, AK 99709

<sup>2</sup> University of Alaska Fairbanks, Arctic Coastal Geoscience Lab, P.O. Box 755780, Fairbanks, AK 99775

\*2025 Update – Drone video added

## METHODS

### Aerial Photogrammetric Survey Details

DGGS conducted flights on June 21, 2022, from approximately 9:00 AM to 5:15 PM AKDT. DGGS used a DJI Phantom 4 RTK UAV with an FC6310R camera model (8.8 mm lens) to collect 3,601 megapixel JPEG photographs (5,472 x 3,648 pixels per image). The operator returned the UAV eight times to change the batteries. DGGS flew the aerial survey with 70 percent sidelap and 80 percent frontlap, 100 m above ground level at 7.9 m/s, with the nadir orientation stabilized using a three-axis gimbal. This resulted in images covering 3.603 km<sup>2</sup> with a ground sampling distance (GSD) of 0.020 m. The weather throughout the survey was mostly overcast with light wind. No abnormalities were observed during the flights.

### Ground Survey Details

On June 21, 2022, DGGS set up a Global Navigation Satellite System (GNSS) base station using a Trimble R10 receiver sampling at 5 Hz over a found stainless steel rod in a lidded case. This provided real-time kinematic (RTK) corrections to the ground rover, a Trimble R8s GNSS receiver. DGGS measured the location of 25 photo-identifiable ground control points (GCPs) with the ground rover (fig. 2).

### Data Processing

Base positions were corrected using Online Positioning User Service (OPUS) solutions (table 1), which were used to update the UAV and ground rover positions with post-processed kinematic (PPK) adjustments.

UAV positions were updated in RTKLIB (Version 2.4.3) software with the following settings applied: L1+L2 frequencies forward and backward filtered; a 10° elevation mask; receiver dynamics disabled; broadcast ionosphere and Saastamoinen troposphere corrections; a minimum fixed-ambiguity ratio of three; and L1/L2 code/carrier-phase error ratios of 100. During post-processing, DGGS applied International GNSS Service (IGS) precise orbits and final clock solutions retrieved from the Crustal Dynamics Data Information System (CDDIS) found at [urs.earthdata.nasa.gov/](https://urs.earthdata.nasa.gov/). Final corrected data were exported as time-stamped position files in the WGS84 horizontal coordinate system with ellipsoidal heights and paired to corresponding photographs using an Aerotas P4RTK PPK Adjustments (Version 1) macro-enabled Microsoft Excel file.

Ground rover positions were updated using PPK corrections in Trimble Business Center (Version 5.51) software using default settings. The final corrected data were exported as comma-delimited text files in the WGS84 horizontal coordinate system with ellipsoidal heights.

DGGS used Agisoft Metashape Professional (Version 1.8.3 build 14331) software for photogrammetric processing following the steps and settings outlined in United States Geological Survey (USGS) Open-File Report 2021-1039 (Over et al., 2021). During processing, DGGS used 13 GCPs for photograph alignment and lens distortion parameter optimization (fig. 2, table 2), leaving 12 GCPs as horizontal and vertical check points (fig. 2, table 3). A confidence filter was



applied to the resulting dense point cloud, eliminating all points derived from fewer than three discrete camera positions. Additional noise was removed from the dense point cloud through visual inspection.

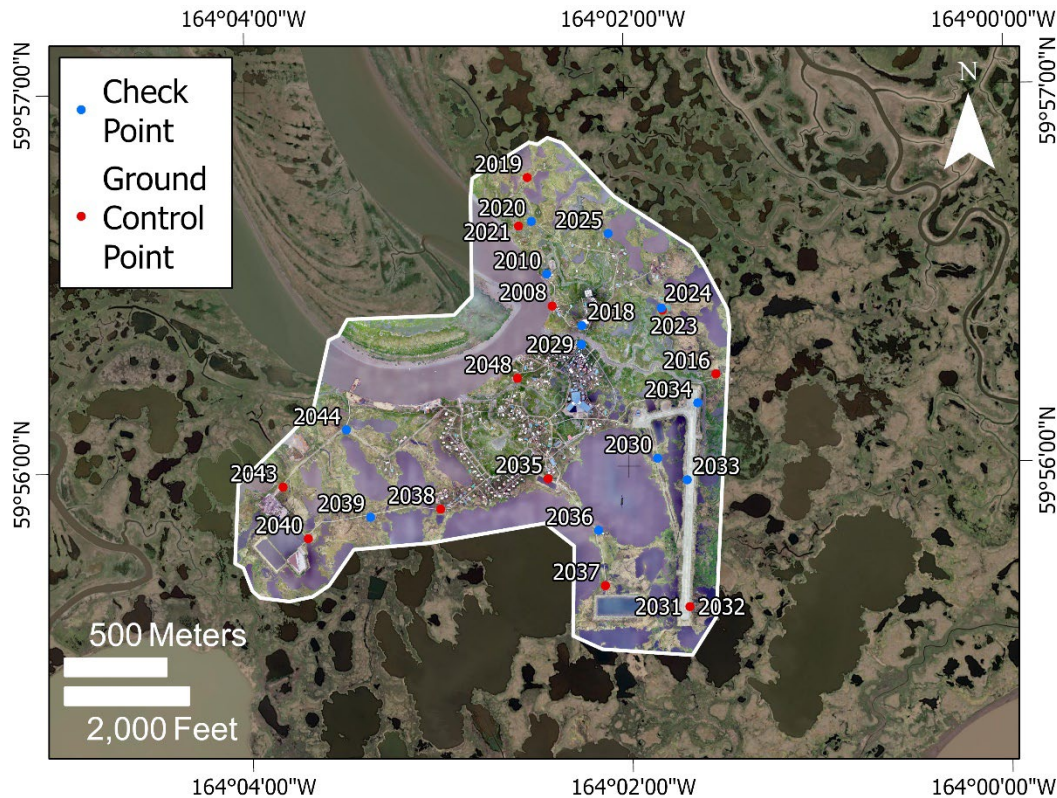


**Figure 2.** Location of photo-identifiable ground control points (GCP; red) and check points (CHK; blue).

## IMAGERY PRODUCTS

### Orthoimagery

The orthoimage is a three-band (red, green, blue), eight-bit unsigned GeoTIFF file derived from a color adjusted mosaic of 3,519 aerial photographs with a GSD of 0.020 m per pixel; the “No Data” value is set to 0.

### Digital Surface Model

The DSM represents surface elevations including the height of vegetation, buildings, and other man-made features derived from the dense point cloud. The DSM is a single-band, 32-bit floating point GeoTIFF file with a GSD of 0.055 m; the “No Data” value is set to  $-3.4028235 \times 10^{38}$ .

## ACCURACY REPORT

### Coordinate System and Datum

All data were processed in the WGS84 horizontal coordinate system and WGS84 ellipsoid vertical datum. All data were reprojected using Esri ArcGIS Pro (Version 3.0.2) software and are delivered in NAD83 (2011) UTM Zone 3N horizontal coordinate system and NAVD88 (GEOID12B) vertical datum.

### Horizontal Accuracy

DGGS quantified the horizontal accuracy of the GNSS position data using the latitudinal and longitudinal peak-to-peak errors provided by OPUS (table 1). Consistent with OPUS shared solution requirements (NOAA, 2022), DGGS considers high-quality GNSS solutions to have latitudinal and longitudinal errors less than or equal to 0.04 m.

We quantified the horizontal accuracy of the DSM and orthoimage by comparing the known locations of 12 photo-identifiable check points measured with GNSS against their modeled locations in the photogrammetric products (fig. 2, table 3). These are independent checkpoints not used during processing. X and Y errors are calculated as the root-mean-square (RMS) error of offsets, 0.044 m and 0.031 m, respectively. The total horizontal error is the root-sum-square error of X and Y RMS errors, 0.054 m.

### Vertical Accuracy

DGGS quantified the vertical accuracy of the GNSS position data using the combined ellipsoidal height peak-to-peak errors provided by OPUS and orthometric height RMS error provided by NOAA's Vertical Datum Transformation software (NOAA, 2016; table 1). Consistent with OPUS shared solution requirements (NOAA, 2022), DGGS considers high-quality GNSS solutions to have vertical errors less than or equal to 0.08 m.

We quantified the DSM's vertical accuracy using the same 12 check points used to quantify the horizontal accuracy (fig. 2, table 3). The RMS error of Z offsets is 0.016 m, and the total RMS error of the DSM (X, Y, and Z) is 0.056 m.

**Table 1.** Base station coordinates and GNSS errors.

NAD83 (2011) Easting	NAD83 (2011) Northing	NAVD88 Elevation	GNSS X Error (m)	GNSS Y Error (m)	GNSS Z Error (m)
554135.137	6644568.574	4.451	0.008	0.011	0.077

**Table 2.** Ground control point coordinates and offsets from orthoimagery and DSM.

Point	Easting	Northing	Elevation	X Offset (m)	Y Offset (m)	Z Offset (m)	GNSS X/Y Error (m)	GNSS Z Error (m)
2008	6645167.884	553648.648	2.935	0.020	-0.061	0.005	0.013	0.016
2016	6644834.108	554451.703	3.350	-0.045	0.043	-0.024	0.004	0.007
2019	6645797.378	553526.840	3.464	-0.018	0.041	0.029	0.007	0.011
2021	6645559.171	553483.465	2.866	-0.009	0.021	0.007	0.007	0.011
2023	6645148.132	554188.389	3.690	-0.019	0.037	0.023	0.006	0.009
2031	6643694.300	554325.412	4.559	-0.049	-0.025	-0.021	0.005	0.007
2032	6643693.595	554325.252	4.565	-0.032	-0.004	-0.033	0.006	0.008
2035	6644321.097	553629.309	4.084	-0.050	-0.027	-0.017	0.006	0.009
2037	6643797.027	553910.159	3.142	-0.015	0.007	-0.002	0.007	0.009

Point	Easting	Northing	Elevation	X Offset (m)	Y Offset (m)	Z Offset (m)	GNSS X/Y Error (m)	GNSS Z Error (m)
2038	6644171.520	553100.697	3.005	-0.017	-0.040	0.003	0.008	0.009
2040	6644025.978	552451.043	4.447	0.016	-0.004	-0.022	0.009	0.010
2043	6644279.526	552327.718	3.041	0.026	0.012	-0.004	0.009	0.010
2048	6644813.094	553477.799	3.163	0.031	-0.006	0.004	0.009	0.012
<b>Mean</b>				-0.012	0.000	-0.004	0.007	0.010
<b>Standard Deviation</b>				0.028	0.032	0.019	0.002	0.002
<b>Range</b>				0.082	0.105	0.062	0.009	0.009
<b>Root Mean Square Error</b>				0.027	0.031	0.018	0.002	0.002
<b>Total Error</b>				<b>0.041</b>		<b>0.045</b>	<b>0.003</b>	
				<b>(XY)</b>		<b>(XYZ)</b>	<b>(XYZ)</b>	

**Table 3.** Check point coordinates and offsets from orthoimagery and DSM.

Check Point	Easting	Northing	Elevation	X Offset (m)	Y Offset (m)	Z Offset (m)	GNSS X/Y Error (m)	GNSS Z Error (m)
2010	553621.194	6645323.995	3.246	0.020	-0.021	0.032	0.010	0.012
2018	553793.585	6645071.995	3.221	0.137	0.079	0.013	0.005	0.008
2020	553545.828	6645582.067	2.700	-0.030	-0.020	0.028	0.007	0.011
2024	554184.166	6645156.742	3.637	-0.035	0.025	0.009	0.007	0.010
2025	553922.232	6645522.334	2.673	0.013	0.039	-0.013	0.008	0.011
2029	553792.334	6644978.014	3.644	-0.030	-0.016	0.024	0.012	0.014
2030	554165.531	6644421.703	4.896	-0.011	-0.034	-0.009	0.013	0.016
2033	554311.625	6644316.307	5.168	-0.013	-0.002	-0.019	0.006	0.008
2034	554362.373	6644692.294	4.993	-0.028	0.041	0.004	0.006	0.008
2036	553876.586	6644067.562	2.937	0.011	0.012	-0.013	0.007	0.009
2039	552756.343	6644132.513	3.054	0.004	0.011	0.007	0.008	0.010
2044	552637.483	6644559.756	3.648	-0.011	0.004	0.013	0.009	0.010
<b>Mean</b>				0.002	0.010	0.006	0.008	0.010
<b>Standard Deviation</b>				0.046	0.032	0.017	0.002	0.003
<b>Range</b>				0.172	0.112	0.051	0.008	0.009
<b>Root Mean Square Error</b>				0.044	0.031	<b>0.016</b>	0.002	0.002
<b>Total Error</b>				<b>0.054</b>		<b>0.056</b>	<b>0.003</b>	
				<b>(XY)</b>		<b>(XYZ)</b>	<b>(XYZ)</b>	

**Data Consistency and Completeness**

DGGS visually inspected the orthoimage for data errors such as shifts, seamline mismatches, and water noise overlapping land. Visual errors common to these SfM photogrammetry products

include discontinuous powerlines and distortion near high-angle features like buildings and water boundaries. Highly reflective objects such as water bodies, metal roofs, and white paint may cause overexposure, leading to spurious elevation points. There were no significantly erroneous areas that required repair.

## **ACKNOWLEDGMENTS**

We thank the Native Village and City of Kipnuk for supporting the creation of these data products, made possible with National Fish and Wildlife Foundation's National Coastal Resilience Funding through our partners at the Alaska Native Tribal Health Consortium. The views and conclusions contained in this document are those of the authors and should not be interpreted as representing the opinions or policies of the Alaska Division of Geological & Geophysical Surveys, the U.S. Government, or the National Fish and Wildlife Foundation and its funding sources. Mention of trade names or commercial products does not constitute their endorsement by the Alaska Division of Geological & Geophysical Surveys, the U.S. Government, or the National Fish and Wildlife Foundation and its funding sources.

## **REFERENCES**

- National Oceanic and Atmospheric Administration (NOAA), 2016, Estimation of vertical uncertainties in VDatum, [https://vdatum.noaa.gov/docs/est\\_uncertainties.html](https://vdatum.noaa.gov/docs/est_uncertainties.html)
- 2022, About OPUS, retrieved from <https://geodesy.noaa.gov/OPUS/about.jsp>.
- Over, J.R., Ritchie, A.C., Kranenburg, C.J., Brown, J.A., Buscombe, D., Noble, T., Sherwood, C.R., Warrick, J.A., and Wernette, P.A., 2021, Processing coastal imagery with Agisoft Metashape Professional Edition, version 1.6—Structure from motion workflow documentation: U.S. Geological Survey Open-File Report 2021-1039, 46 p., <https://doi.org/10.3133/ofr20211039>.